

Enhancement of the density of states at the Fermi level due to oxygen atoms in noble metals

Sudipta Roy Barman¹ and Aparna Chakrabarti^{2,3}

¹UGC-DAE Consortium for Scientific Research, Khandwa Road, Indore, 452001, Madhya Pradesh, India

²Theory and Simulations Laboratory, Raja Ramanna Centre for Advanced Technology, Indore, 452013, India and

³Homi Bhabha National Institute, Training School Complex, Anushakti Nagar, Mumbai, 400094, India

The interaction of oxygen with noble metals such as silver has been an important topic of research for many decades. Here, we show occurrence of a peak in the density of states (DOS) at the Fermi level (E_F) when oxygen atoms occupy disordered substitutional positions in noble metals such as Ag, Au or Ag-Au alloy. This results in large enhancement of DOS at E_F with respect to Ag or Au metal. Its origin is attributed to O $2p$ related disorder broadened flat band that straddles almost all the high symmetry directions of the Brillouin zone. Our work suggests that if a large concentration of disordered oxygen can be realized in nano-structures of noble metals, it may lead to interesting phenomenon.

Introduction:

From way back, the interaction of oxygen with noble metals such as silver has fascinated scientists through different intriguing phenomena such as high solubility of oxygen in liquid Ag that changes its freezing point[1], dissociation of oxygen molecule at the silver surface[2], incorporation of oxygen atoms (O-atoms) in the bulk[3–6] enhancing its catalytic activity[7, 8], elongation of free standing silver atom chain by incorporation of alternate O-atoms[9], and anomalous superconducting proximity effect where Ag layer increases the transition temperature (T_C) of Pb by 15%[10]. Density functional theory (DFT) calculations by Gravil *et al.*[2] showed that oxygen dissociates into chemisorbed atomic species with no barrier, while Li *et al.*[8] showed that O-atoms in Ag are responsible for the catalysis. An experimental study by Bao *et al.*[3] reported that incorporation of O-atoms in the subsurface causes a 3% expansion of the topmost layer. Eberhart *et al.* performed a first-principles calculation of the charge density to find that the transport of O-atoms through the octahedral interstitial sites is favored in Ag and Cu, but not in Au[4]. The authors however did not consider the vacancies, and a later DFT study showed that rather than existing as an O atom- vacancy pair, the O-atom prefers to occupy the Ag vacancy *i.e.* exist at the substitutional site[5]. Baird *et al.* proposed how an O-atom would diffuse in Ag by absorbing a phonon to overcome the potential energy barrier[6]. Among the different types of O-atoms that were identified in Ag, O_β is the bulk dissolved oxygen, while O_γ is a strongly bound species[7]. The stoichiometric oxides of Ag are semiconducting and these have been studied by DFT primarily to understand why high T_C superconductivity is absent in Ag oxides in spite of their similarity with the Cu oxides[11, 12].

Compared to the bulk, Ag nano-particles (NP) are more susceptible to oxidation[13, 14]. Large concentrations of O and C (0.55 and 5 times, respectively with respect to Ag) in Ag@Au core-shell particles (where Ag is the core and Au is the shell) have been reported from x-

ray photoelectron spectroscopy (XPS)[14]. Significantly, the oxygen and carbon signals increase for XPS measurement performed in the bulk sensitive mode, indicating that these are present primarily within the NP and not at the surface. A detailed work using x-ray absorption fine structure spectroscopy and molecular dynamics by Shibata *et al.* showed existence of vacancies in Au@Ag NP at room temperature that facilitates interface alloying[15]. A scanning tunneling microscopy study showed that with application of electrochemical potential, vacancy clusters can grow and diffuse on Ag-Au alloy[16]. This effect is pronounced for small particles of size less than 4.6 nm, where the two metals are nearly randomly distributed. Recently, Yue *et al.* have demonstrated by transmission electron microscopy and theoretical simulation that oxygen molecules dissociate on the surface of silver NP and diffuse through them to reach the silver/carbon interface and eventually oxidize the carbon[17]. The lattice distortion caused by oxygen concentration gradient within the silver nanoparticles provides the direct evidence for oxygen diffusion.

In this work, we investigate how the electronic structure of fcc noble metals such as Ag and Au is modified by O-atoms in the disordered substitutional (*i.e.* O-atoms in metal vacancy positions) and interstitial positions using the spin polarized fully relativistic Korringa Kohn Rostoker (SPRKKR) method[18]. For O-atoms in the substitutional position, we find a huge increase in the density of states (DOS) at the Fermi level (E_F) caused by a sharp peak related to O $2p$ -like states. The Bloch spectral function, which is the counterpart of dispersion relation for an ordered solid, shows flat and narrow regions straddling the Fermi level along almost all the high symmetry directions of the Brillouin zone (BZ). This is similar to a flat band in an ordered solid that has been broadened by disorder. We show that this phenomenon also occurs in Au, as well as Ag-Au alloy. We hence argue that in nano-structures, presence of disordered oxygen bound by dispersive force and stabilized by the noble metal matrix might lead to enhancement of conductivity.

Methods:

We have performed self-consistent band structure calculations using SPRKKR method in the atomic sphere approximation[18] within the generalized gradient approximation[19]. The site disorder was treated by coherent potential approximation (CPA) that calculates the configurationally averaged electronic structure self consistently within a mean-field theory. In general, CPA focuses on understanding the scattering of electrons in a material which exhibits spatial inhomogeneity and has turned out to be the most well established way of calculating the influence of disorder on the electronic properties of different materials. The angular momentum expansion up to $l_{max} = 4$ has been used for each atom. The energy convergence criterion and CPA tolerance has been set to 10^{-5} Ry. BZ integrations were performed on a $45 \times 45 \times 45$ mesh of k -points in the irreducible wedge of the BZ. We have also carried out spin polarized calculations within the SPRKKR formalism. However, we arrive at converged SCF results where the systems turn out to be non-magnetic *i.e.* the atoms do not carry any partial moment, although the magnetic moments were $0.01\mu_B$ for Ag and as large as $1\mu_B$ for O in the starting configuration for all the different Ag/Au-O calculations presented here.

The supercell calculation with full potential linearized augmented plane wave method[20] has been performed with 8000 k points in BZ (256 k points in the irreducible BZ). The energy cut-off is about 14.5 Ry and the tolerance for energy convergence is 10^{-4} Ry. The cohesive energy (E_{coh}), for example for Ag_mO_n , has been calculated using $E_{coh} = E_{tot}(Ag_mO_n) - m \times E_{tot}(Ag) - n \times E_{tot}(O)$, where $E_{tot}(Ag_mO_n)$, $E_{tot}(Ag)$ and $E_{tot}(O)$ are the total energies of the concerned Ag_mO_n system, Ag and O atoms, respectively. It may be noted that since it is uncertain to which components Ag_mO_n might possibly convert to, its stability against the decomposition into stoichiometric oxide (Ag_2O , AgO , or Ag_2O_3) and O_2 phases is not addressed in this work.

Results and Discussion:

The total and partial density of states (PDOS) of Ag with different amounts of randomly substituted O-atoms are shown in Fig. 1(a-e). The calculations are performed using the equilibrium lattice constant (a_{eq}) obtained by fitting the variation of the total energy as a function of lattice constant using a polynomial function.

In all cases, a_{eq} turns out to be within a few percent of the Ag lattice constant (4.085\AA). A broad hump centered around -0.7 eV in the total DOS of $Ag_{88}O_{12}$ that is absent in Ag originates from the O $2p$ -like states Fig. 1(a,b). This feature causes an enhancement of the DOS at E_F (n_F) by 46% compared to Ag. The intensity of the hump increases in $Ag_{75}O_{25}$, and it shifts very close to E_F (-0.2 eV). It is striking to note that, for $Ag_{60}O_{40}$, this O $2p$ related peak becomes narrower and appears at E_F , caus-

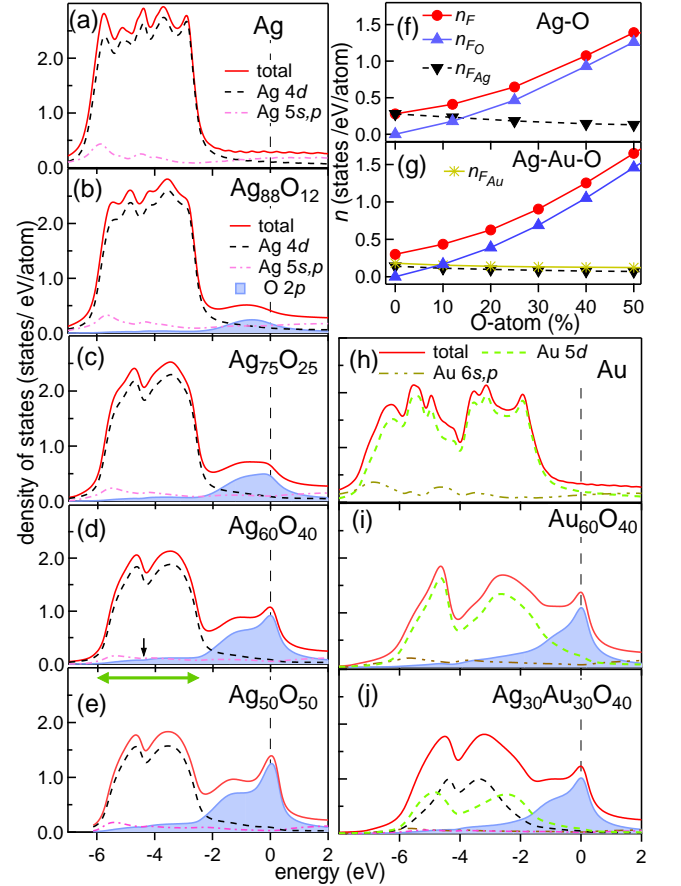


Figure 1: Total and partial density of states of (a) Ag, (b) $Ag_{88}O_{12}$, (c) $Ag_{75}O_{25}$, (d) $Ag_{60}O_{40}$, (e) $Ag_{50}O_{50}$, (h) Au, (i) $Au_{60}O_{40}$, and (j) $Ag_{30}Au_{30}O_{40}$. The total DOS at E_F (n_F) and the total Ag ($n_{F_{Ag}}$), O (n_{F_O}) and Au ($n_{F_{Au}}$) contributions to n_F for (f) Ag-O (g) Ag-Au-O, as a function of O-atom content.

ing a very large increase of n_F by 286% (Fig. 1(d,f)). This effect is even more pronounced for $Ag_{50}O_{50}$, with a 400% increase of n_F , with the maximum of the O $2p$ PDOS peak right at E_F (Fig. 1(e,f)). The enhancement of n_F is also obtained for Au-O (Fig. 1(h,i)), as well as in Ag-Au-O (Fig. 1(g,j)). In fact, for the same oxygen content, n_F is largest in Au-O (*e.g.* $n_F = 1.37$ states/eV/atom for $Au_{60}O_{40}$ in Fig. 1(i)), compared to $n_F = 1.25$ states/eV/atom for $Au_{30}Ag_{30}O_{40}$ in Fig. 1(j) and $n_F = 1.07$ states/eV/atom for $Ag_{60}O_{40}$ in Fig. 1(d)). For a disordered system, an equivalent of the band dispersion $E(k)$ can be obtained through the Bloch spectral function, $A_B(k, E)$, which is defined as the Fourier transform of the retarded single electron Green's function[21]. For an ordered system, Bloch spectral function (BSF) reduces to a set of δ functions at the band energies giving $E(k)$. With introduction of disorder, these δ -function peaks are broadened. To find the origin of the DOS peak at E_F in Fig. 1, we have calculated the BSF

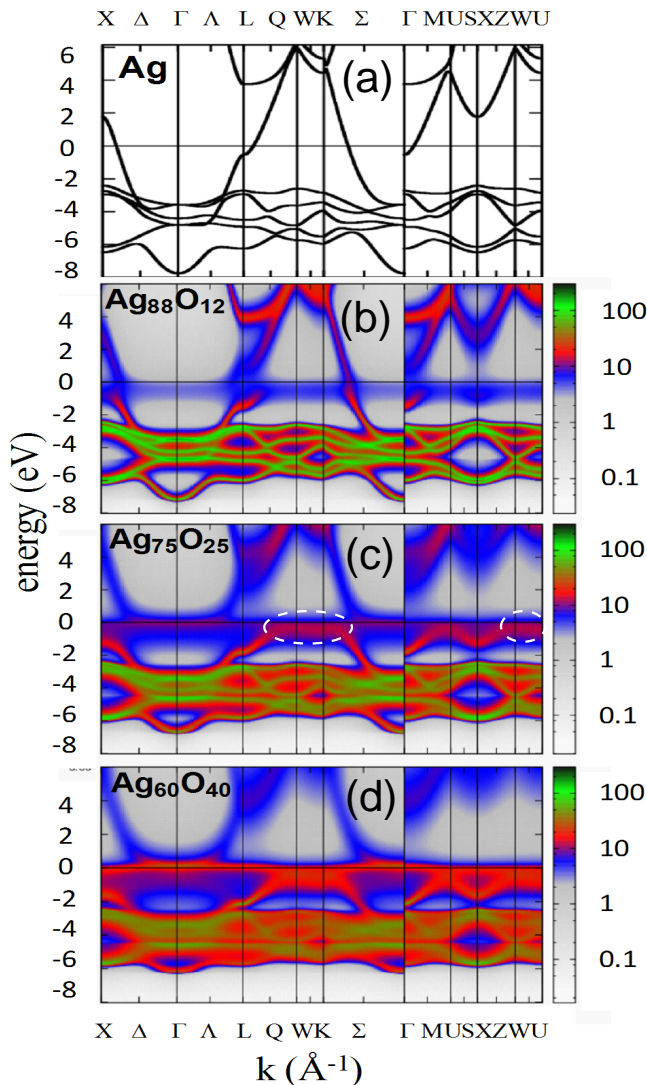


Figure 2: (a) The band dispersion $E(k)$ along the different high symmetry directions of Ag compared with the Bloch spectral function $A_B(k, E)$ along the same directions for (b) $\text{Ag}_{88}\text{O}_{12}$, and (c) $\text{Ag}_{75}\text{O}_{25}$, and (d) $\text{Ag}_{60}\text{O}_{40}$, the color scale on the right side shows the values of $A_B(k, E)$ in a.u.

along the high symmetry directions of the fcc BZ. If the BSF of $\text{Ag}_{88}\text{O}_{12}$ in Fig. 2(b) is compared to $E(k)$ of Ag (Fig. 2(a)), it is observed that the dispersing Ag s, p band with a kink at the L point splits in the former. The splitting happens because the occupied band shifts down in energy to about -1.5 eV, while the unoccupied part up to 1 eV diminishes in intensity (in Fig. 2(b) see the red colored band around L point, red is about 25 in the relative intensity logarithmic color scale with green as maximum (≈ 100) and white as minimum (zero)). The same happens for the other dispersing Ag $s-p$ bands, e.g. the bands crossing E_F at middle of $\Delta-X$ and near M point. Thus, evidently, the contribution of Ag $s-p$ states to n_F

decreases. A curious observation from Fig. 2(b) is the appearance of states of low intensity at E_F (blue region, 5 in the intensity scale) and we examine how these evolve with larger O-atom content. Strikingly, for $\text{Ag}_{75}\text{O}_{25}$ in Fig. 2(c), parts of the blue region become intense and appear as flat red bands along $W-U$ and $Q-\Sigma$ (both encircled by white dashes). The flat band along $Q-\Sigma$ connects two dispersing bands crossing L and Σ . A parabolic band emerges with minimum at X at -1.5 eV and disperses up to the flat band along $W-U$. Weak flat bands (light red color) at E_F is also observed along $\Delta-\Gamma-\Lambda$ and $\Sigma-\Gamma$. A spectacular effect occurs for $\text{Ag}_{60}\text{O}_{40}$ (Fig. 2(d)): a flat narrow band (red color) appears at E_F spanning all the high symmetry directions from $X-\Gamma-L-W-K-\Gamma$ and $\Gamma-U-X-W-U$ that we have calculated (encircled by yellow dashes). The very wide k range of the flat band, as if it is ubiquitous, along the different directions of the fcc BZ is completely unique. Obviously, this is the origin of the sharp DOS peak at E_F . The intensity of this flat band further increases for $\text{Ag}_{50}\text{O}_{50}$. The BSF curves of $\text{Au}_{60}\text{O}_{40}$ and $\text{Au}_{30}\text{Ag}_{30}\text{O}_{40}$ also show presence of this intense flat band at E_F (Fig.3).

In order to further understand why presence of O-atoms in Ag or Au causes such a large enhancement of the DOS at E_F , we find from the integration of the PDOS up to E_F that the total valence charge in O-atom varies from 4.4 to 4.6 *i.e.* its valency being -0.4 to -0.6 . Thus, the O-atom is almost neutral, with a small excess negative charge ($2p^4$ is the valence configuration of oxygen). Its valency is remarkably smaller than the nominal valency of -2 for oxygen, for example, in stoichiometric oxides, where the covalent bonding is predominant and Ag to O nearest neighbor (nn) distance is $\approx 2\text{\AA}$ [12]. On the other hand, in Ag/Au-O systems studied here, the nn distance between two O-atoms is substantially larger (e.g. 2.84\AA for $a_{eq} = 4.02\text{\AA}$) and thus orbital overlap required for covalent bonding is diminished. Rather, it is interesting to note that the van der Waals (vdW) diameter of the O-atom, *i.e.* the distance between two O-atoms where the minimum of the Lennard-Jones interaction potential occurs, is reported from different estimates to be in the range of 2.8\AA to 3\AA [22, 23]. Thus, based on the observations that the O-atoms are almost neutral and at a distance equivalent to their vdW diameter, the dominance of vdW bonding between O-atoms is expected.

In Fig. 1, the O $2p$ states extend from E_F to -6 eV; it has a shoulder at -1.3 eV that arises mainly from the $2p_{x,y}$ states, while the peak at E_F has similar contributions from all the three p components. Its noteworthy that in the -2.5 to -6 eV region (e.g. indicated by green horizontal arrow in Fig. 1(d)), the O $2p$ PDOS tails out as almost flat with apparently low intensity, but in reality it constitutes about 20% of the total occupied PDOS. It has a similarity of shape with the Ag d states, with both exhibiting a minima at -4.5 eV (black arrow). Such tailing of the O $2p$ PDOS is also observed for $\text{Au}_{60}\text{O}_{40}$ and

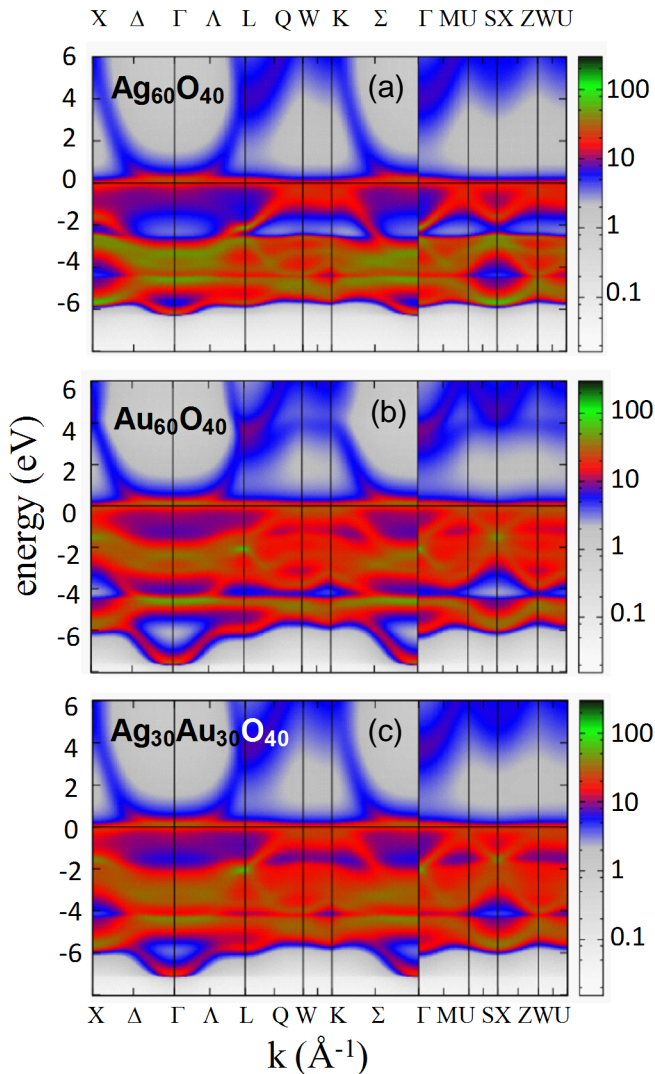


Figure 3: A comparison of the Bloch spectral function $A_B(k, E)$ along the different high symmetry directions of the fcc BZ (a) $\text{Ag}_{60}\text{O}_{40}$, (b) $\text{Au}_{60}\text{O}_{40}$, and (c) $\text{Ag}_{30}\text{Au}_{30}\text{O}_{40}$; the color scale on the right side shows the values of $A_B(k, E)$ in a.u. A high intensity of $A_B(k, E)$ at E_F is observed in all cases resembling a disorder broadened flat band.

$\text{Ag}_{30}\text{Au}_{30}\text{O}_{40}$ (Fig. 1(i,j)), indicating hybridization of the O $2p$ states with the noble metal d states. The cohesive energies (E_{coh}) of $\text{Ag}_{60}\text{O}_{40}$ and $\text{Au}_{60}\text{O}_{40}$ have been calculated by considering a $2 \times 2 \times 2$ fcc supercell of 32 atoms with random configurations of 13 O-atoms using full potential linearized augmented plane wave (FPLAPW) method[20]. The DOS shows the O $2p$ related sharp peak at E_F (Fig. 4), which is of similar intensity as in Fig. 1(d). The PDOS also has the hump around -1.3 eV and the flat DOS region. However, the DOS in this case is highly structured; this is because here we have considered only one particular configuration of O-atoms that is repeated in space in the FPLAPW method and

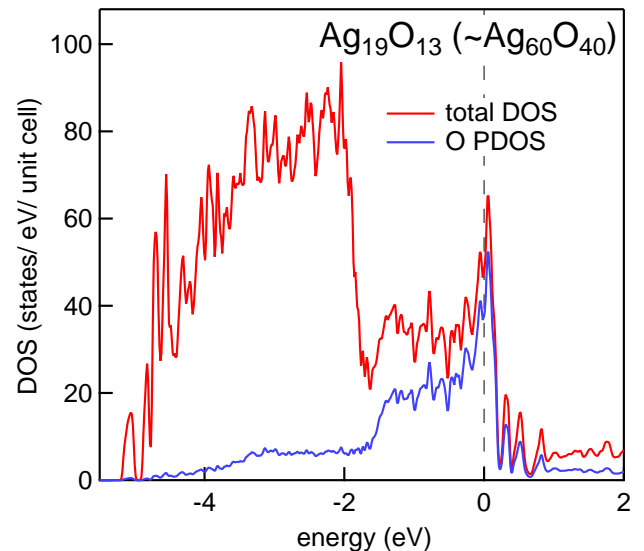


Figure 4: The total and oxygen density of states for $\text{Ag}_{19}\text{O}_{13}$ (~ $\text{Ag}_{60}\text{O}_{40}$) calculated with a 32 atom fcc supercell using full potential linearized augmented plane wave method.

thus it is not a fully disordered structure. The values of E_{coh} for $\text{Ag}_{60}\text{O}_{40}$ and $\text{Au}_{60}\text{O}_{40}$ are 2.8 eV/atom and 2.9 eV/atom, respectively. In comparison, E_{coh} for O in fcc structure with same lattice constant is much smaller (1.3 eV/atom). Thus, hybridization of O $2p$ and the Ag/Au d states, as well as their cohesive energies indicate the importance of the noble metal matrix in providing the stability.

We have also considered O-atoms to be randomly distributed in octahedral and tetrahedral interstitial positions of Ag (Fig. 5(b,c)), since these have been reported in literature as possible sites that oxygen could occupy[4–6]. In both the interstitial positions, due to the close proximity of O and Ag atoms (2.04 Å for octahedral and 1.77 Å for tetrahedral sites), the Ag $4d$ -O $2p$ hybridization dominates and the Ag $4d$ PDOS is largely modified. The O $2p$ PDOS exists over a wide energy range of 10-12 eV, and does not have any peak at E_F . Nevertheless, n_F increases moderately with O-atom content (Fig. 5(a)). In contrast to Ag-O (Fig. 1), this is caused primarily by Ag $4d$ and $5s, p$ states rather than O $2p$ states.

A recent work claimed occurrence of room temperature superconductivity in 10Å Ag NP in Au matrix[24], although it must be mentioned at the onset that reproducibility of the data has not been established in the literature yet[25]. It is well-known that high temperature superconductivity could be achieved in materials with large n_F and high Debye temperature, however, claim of superconductivity in pure Ag@Au nano-structure (NS) is very curious and even seems unrealistic, since neither Ag nor Au are superconducting. In Ref. 24, the au-

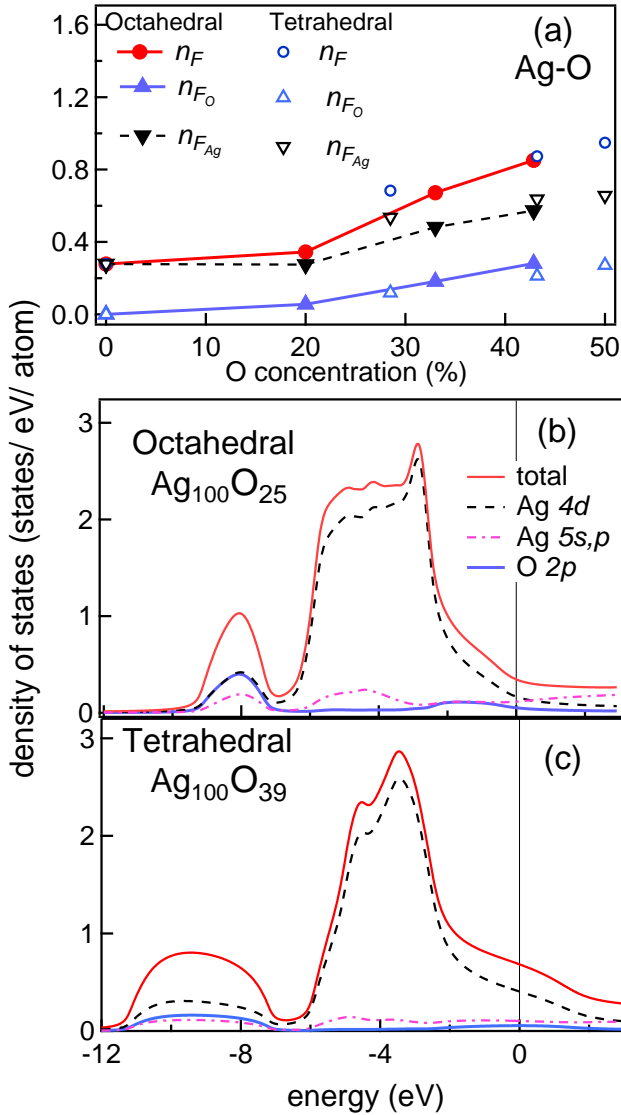


Figure 5: (a) The total DOS at E_F (n_F) and the total Ag ($n_{F_{Ag}}$) and O (n_{F_O}) contributions to n_F for O-atoms in octahedral and tetrahedral interstitial positions, as a function of O-atom concentration. Total density of states, Ag 4d, Ag 5s,p and O 2p PDOS for (b) octahedral $Ag_{100}O_{25}$ and (c) tetrahedral $Ag_{100}O_{39}$, where disordered O-atoms and vacancies are considered in the interstitial sites.

thors did not discuss the amount of oxygen present in the Ag@Au NS, although their EDAX data show presence of C and O $K\alpha$ peaks at 0.28 and 0.53 keV, respectively. It is well known in literature that Ag NP are prone to oxidation[13, 14] and the following estimate provides an idea about possible oxygen content: in a 10 Å Ag NP, there are about 30 atoms. If a single O-atom layer is considered to fully cover this spherical NP, an estimate of the number of O-atoms considering these as hard spheres with atomic diameter of 1 Å will involve 400 O-atoms. The x-ray diffraction pattern shows that the Ag@Au NS

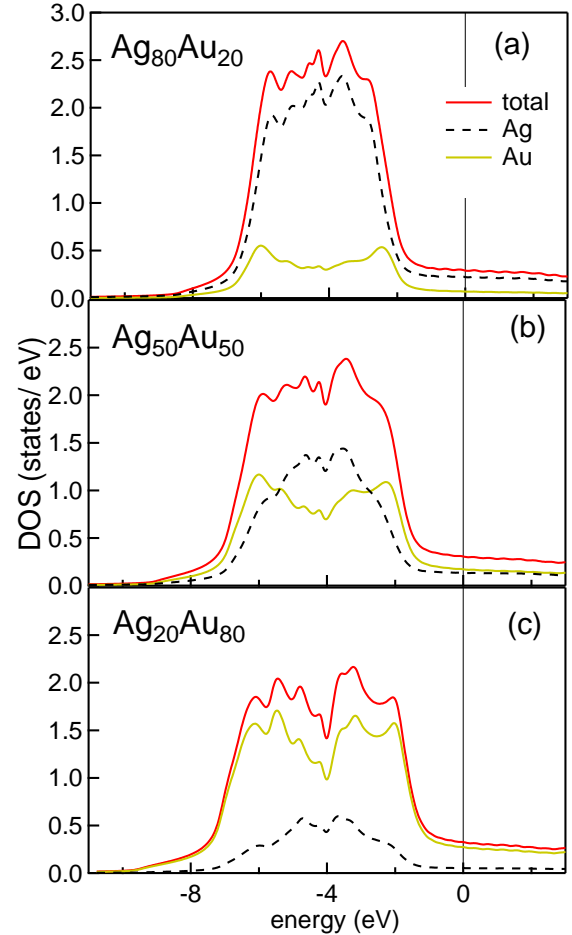


Figure 6: The total, Ag and Au density of states for (a) $Ag_{80}Au_{20}$, (b) $Ag_{50}Au_{50}$ and (c) $Ag_{20}Au_{80}$. The position of the Ag 4d and Au 5d states remain essentially unchanged and their relative intensities vary proportionately with composition, with hardly any modification in the DOS of the s,p states at E_F .

has fcc structure with no extra phases[24]. This shows that the oxygen present in the NS does not form any of the known oxides of Ag since their structures are not fcc. This indicates that the O-atoms in the NS are present in disordered positions that keep the fcc structure unaffected. We further point out that the O-atoms could be present in the Ag vacancy (*i.e.* substitutional) sites from the evidences provided by Shibata *et al.*[15], Oppenheim *et al.*[16] and Yue *et al.*[17], who establish presence of vacancies and O-atoms, their migration through the NP and complete alloying, particularly in small NP of size less than 46 Å. Moreover, a DFT study by Crocombette *et al.* established that it is energetically favored for an oxygen-vacancy pair in Ag to transform to a substitutional O-atom[5]. On the basis of the above arguments, it is conceivable that there is a probability that O-atoms can form local regions of disordered Ag/Au-O with high

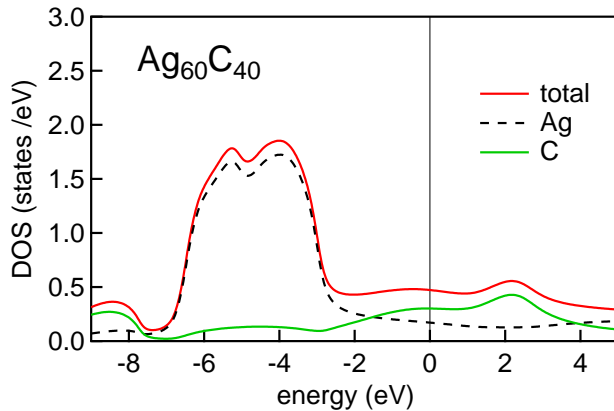


Figure 7: (a) The total, Ag and C density of states for $\text{Ag}_{60}\text{C}_{40}$, where C is in disordered substitutional positions. The calculation has been performed using optimized lattice constant (3.922 Å). A peak in the C 2p PDOS appears above E_F at 2.2 eV.

oxygen concentration encompassing the Ag core and Au matrix, thus possibly forming a connected pathway of regions of high DOS at the Fermi level resulting in high conductivity. While the large DOS at the Fermi level due to occurrence of disordered broadened flat bands as observed in Figs. 1-3 may favor superconductivity[26–28], whether indeed the local oxygen induced superconducting regions may be formed in this kind of systems needs to be probed experimentally.

We also probe the possibility of alloying of Ag with Au in an Ag-Au alloy. In Fig. 6, we show the DOS of site-disordered Ag-Au alloys with composition varying from $\text{Ag}_{80}\text{Au}_{20}$ to $\text{Ag}_{20}\text{Au}_{80}$. Neither any enhancement of n_F nor transfer of charge from Ag to Au is observed from our SPRKKR calculation. We have also considered disordered carbon in Ag (Ag-C), as carbon has been observed to be present in the EDAX signal of Ag@Au NS[24]. The DOS of $\text{Ag}_{60}\text{C}_{40}$ in Fig. 7 calculated using optimized lattice constant of 3.922 Å does not show any peak at E_F . n_F turns out to be 0.47 states/eV/atom, which although is larger than Ag, is considerably less compared to $\text{Ag}_{60}\text{O}_{40}$.

Conclusion:

We show from density functional theory calculations using SPRKKR method that incorporation of oxygen atoms in disordered substitutional positions of noble metals such as Ag, Au and Ag-Au alloy leads to a large enhancement of the density of states at the Fermi level. The Bloch spectral function, which is the counterpart of dispersion relation for an ordered solid, shows that the peak in the density of states at the Fermi level is related to disorder broadened flat O 2p states that straddle almost all the high symmetry directions of the

Brillouin zone. We argue that large concentration of disordered oxygen atoms, if can be realized in noble metal nano-structures, may result in interesting phenomena and stimulate new experiments on noble metal nano-structures.

Acknowledgments:

We thank the Computer Centre of Raja Ramanna Centre for Advanced Technology, Indore for providing the computational facility. A.C. thanks P.A. Naik for support and encouragement.

-
- [1] E. H. Baker, J. K. Johnstone, *Nature* 205 (1965) 65-66.
 - [2] P. A. Gravil, D. M. Bird, J. A. White, *Phys. Rev. Lett.* 77 (1996) 3933-3936.
 - [3] X. Bao, J. V. Barth, G. Lehmppfuhl, R. Schuster, Y. Uchida, R. Schlögl, G. Ertl, *Surf. Sci.* 284 (1993) 14-22.
 - [4] M. E. Eberhart, M. M. Donovan, R. A. Outlaw, *Phys. Rev. B* 46 (1992) 12744-12747.
 - [5] J.-P. Crocombette, H. de Monestrol, F. Willaime, *Phys. Rev. B* 66 (2002) 024114.
 - [6] J. K. Baird, T. R. King, C. Stein, *J. Phys. Chem. Sol.* 60 (1999) 891-894.
 - [7] A. J. Nagy, G. Mestl, R. Schlögl, *J. Catal.* 188 (1999) 58-68.
 - [8] W.-X. Li, C. Stampfl, M. Scheffler *Phys. Rev. Lett.* 90 (2003) 256102.
 - [9] W. H. A. Thijssen, D. Marjenburgh, R.H. Bremmer, J.M. van Ruitenbeek, *Phys. Rev. Lett.* 96 (2006) 026806.
 - [10] O. Bourgeois, A. Frydman, R.C. Dynes, *Phys. Rev. Lett.* 88 (2002) 186403.
 - [11] Y. Quan, W. E. Pickett, *Phys. Rev. B* 91 (2015) 035121.
 - [12] J.P. Allen, D.O. Scanlon, and G.W. Watson, *Phys. Rev. B* 84 (2011) 115141.
 - [13] C. Shankar, A. T. N. Dao, P. Singh, K. Higashimine, D. M. Mott, S. Maenosono, *Nanotech.* 23 (2012) 245704.
 - [14] I. S.- šloufová, B. Vlčková, Z. Bastl, T. L. Hasslett, *Langmuir* 20 (2004) 3407-3415.
 - [15] T. Shibata, B. A. Bunker, Z. Zhang, D. Meisel, C. F. Vardeman II, J. Daniel Gezelter, *J. Am. Chem. Soc.* 124 (2002) 11989-11996.
 - [16] I. C. Oppenheim, D. J. Trevor, C. E. D. Chidsey, P. L. Trevor, K. Sieradzki, *Science* 254 (1991) 687-689.
 - [17] Y. Yue, D. Yuchi, P. Guan, J. Xu, L. Guo, J. Liu, *Nature Comm.* 7 (2016) 12251.
 - [18] H. Ebert, D. Ködderitzsch, J. Minár, *Rep. Prog. Phys.* 74 (2011) 096501.
 - [19] J. P. Perdew, K. Burke, M. Ernzerhof, *Phys. Rev. Lett.* 77 (1996) 3865-3868.
 - [20] P. Blaha, K. Schwarz, G. K. H. Madsen, D. Kvasnicka and J. Luitz, WIEN2k, (Karlheinz Schwarz, Techn. Universität Wien, Austria), 2001. ISBN 3-9501031-1-2.
 - [21] G. M. Stocks, W. H. Butler, *Phys. Rev. Lett.* 48 (1982) 55-58; H. Ebert, A. Vernes, J. Banhart, *Solid State Comm.* 104 (1997) 243-247; H. Ebert, D. Ködderitzsch, J. Minár, *Rep. Prog. Phys.* 74 (2011) 096501.
 - [22] L. Pauling, *The Nature of the Chemical Bond*, Ithaca: Cornell Univ., (1960)
 - [23] A. Bondi, *J. Phys. Chem.* 68 (1964) 441.

- [24] D. K. Thapa and A. Pandey, arXiv:1807.08572
- [25] B. Skinner, arXiv:1808.02929; N. Singh, arXiv:1808.10388.
- [26] C. C. Tsuei, D. M. Newns, C. C. Chi, P. C. Pattnaik, Phys. Rev. Lett. 65 (1990) 2724-2727.
- [27] G. Li, A. Luican, J. M. B. Lopes dos Santos, A. H. Castro Neto, A. Reina, J. Kong, E. Y. Andrei, Nature Phys. 6 (2010) 109-113.
- [28] Y. Cao, V. Fatemi, S. Fang, K. Watanabe, T. Taniguchi, E. Kaxiras, P. J.-Herrero, Nature 556 (2018) 43-50.